Available online at www.sciencedirect.com
ScienceDirect
Trans. Nonferrous Met. Soc. China 24(2014) 790−797
Transactions of Nonferrous Metals Society of China
www.tnmsc.cn

New numerical algorithm of gas−liquid two-phase flow considering characteristics of liquid metal during mold filling

Xiao-feng NIU[1], Zhao FANG[2], Wei LIANG[1], Hua HOU[3], Hong-xia WANG[1]

1. College of Materials Science and Engineering, Taiyuan University of Technology, Taiyuan 030024, China;
2. School of Metallurgical Engineering, Xi' an University of Architecture & Technology, Xi' an 710055, China;
3. College of Materials Science and Engineering, North University of China, Taiyuan 030051, China

Received 31 May 2013; accepted 18 November 2013

Abstract: A new program is developed for gas−liquid two-phase mold filling simulation in casting. The gas fluid, the superheated liquid metal and the liquid metal containing solid grains are assumed to be governed by Navier–Stokes equations and solved through Projection method. The Level set method is used to track the gas−liquid interface boundary. In order to demonstrate the correctness of this new program for simulation of gas−liquid two-phase mold filling in casting, a benchmark filling experiment is simulated (this benchmark test is designed by XU and the filling process is recorded by a 16-mm film camera). The simulated results agree very well with the experimental results, showing that this new program can be used to properly predicate the gas−liquid two-phase mold filling simulation in casting.

Key words: finite difference method; mold filling process; Projection method; Level set method; two-phase flow; numerical simulation

1 Introduction

The numerical simulation of mold filling is a helpful and important tool for engineers to design casting process [1−13]. Liquid metal often displays complicated behavior and patterns during filling process of casting. For example, the superheated liquid metal has characteristics of incompressible Newtonian flow and the liquid metal containing solid grains and being at lower temperature has characteristics of incompressible non-Newtonian flow. Liquid metal is now often treated as Newtonian flow in some common casting simulation software, and hence unsatisfactory results will be obtained.

The mold filling process is looked as a typical gas−liquid two-phase flow [14−16]. The accurate prediction of some defects, such as the gas entrapment defects, can be achieved by simulating the gas phase flow and the liquid metal phase flow with interface boundary conditions. The Level set method, devised in 1987, has been used and developed in the tracking of the flow front evolution. The Level set method can be used to simulate complex evolution including merging phenomena and breaking without applying reconstruction. Because of these advantages, the Level set method is becoming the most common method for the prediction of interface boundary evolvement.

The SOLA method is often used to solve the velocity and pressure of the thermal flow filling process [15]. The solving process of SOLA method requires repeated iteration between the mass conservation equation and the momentum equations, and hence the computational efficiency is low. The Projection method [17−24] is frequently employed technique for the solution of the Navier−Stokes equations. The Projection method does not need repeated iteration and has high computation efficiency.

In this work, a new program is developed for gas−liquid two-phase mold filling simulation in casting. The gas fluid, the superheated liquid metal and the liquid metal containing solid grains are assumed to be governed by Navier–Stokes equations and solved through Projection method. The Level set method is used to track

Foundation item: Projects (51304145, 51301118, 51304152) supported by the National Natural Science Foundation of China; Project (2013JQ7016) supported by the Natural Science Foundation of Shannxi Province, China; Project (2013T002) supported by the Science Foundation of Taiyuan University of Technology, China; Project (2013JK0904) supported by Shannxi Provincial Education Department, China
Corresponding author: Zhao FANG; Tel: +86-1899194396; E-mail: fangzhao889@126.com
DOI: 10.1016/S1003-6326(14)63127-7

the gas−liquid interface boundary. This proposed program is evaluated by carrying out numerical simulations and by mold filling experimental data.

2 Governing equations

Since the gravity casting processes occur in low speed situations, the compressibility effect of the gas flow can be neglected. Therefore, the gas fluid in the mold is treated as incompressible Newtonian flow.

The theory of gas−liquid two-phase mold filling simulation in casting is discussed based on the computational fluid dynamics (CFD) combined with the finite difference method (FDM). The governing equations for three-dimensional incompressible viscous flow contain the momentum equations and the mass conservation equation (the 3D Cartesian coordinate is used).

The mass conservation equation is written as follows:

$$\frac{\partial u}{\partial x}+\frac{\partial v}{\partial y}+\frac{\partial w}{\partial z}=0 \tag{1}$$

The momentum equation is written as follows:

$$\frac{\partial \boldsymbol{u}}{\partial t}+\nabla\cdot(\boldsymbol{uu})=-\nabla p+\alpha\frac{1}{Re}(\nabla^2\boldsymbol{u})+\beta\nabla\cdot\boldsymbol{S}+\frac{1}{Fr^2}\boldsymbol{g} \tag{2}$$

where $\boldsymbol{u}=(u, v, w)$, t, p, ρ and $\boldsymbol{g}=(g_x, g_y, g_z)$ represent velocity field, time, pressure, density and gravity respectively; $\boldsymbol{S}$ is the non-Newtonian part of the extra stress tensor; $Fr=u_0/\sqrt{gL}$, $Re=\rho u_0 L/\mu$ are the Froude and Reynolds numbers (L and u_0 denote "typical" length and velocity, respectively); μ is the dynamic viscosity.

In order to solve Eq. (1) and Eq. (2), the staggered mesh is established. Because the superheated liquid metal and the gas phase are treated as incompressible Newtonian flow, $\boldsymbol{S}=0$ ($\alpha=1$ and $\beta=0$). The liquid metal containing solid grains is treated as incompressible non-Newtonian flow, $\boldsymbol{S}\neq 0$, so it can be achieved by setting $\alpha=\lambda_2/\lambda_1$, $\beta=1$ (λ_1 and λ_2 are relaxation and retardation time constants).

According to Eq. (1) and Eq. (2), the general mathematical equations of the superheated liquid metal and the gas phase can be written as

$$\nabla\cdot\boldsymbol{u}=0 \tag{3}$$

$$\frac{\partial \boldsymbol{u}}{\partial t}+\nabla\cdot(\boldsymbol{uu})=-\nabla p+\frac{1}{Re}(\nabla^2\boldsymbol{u})+\frac{1}{Fr^2}\boldsymbol{g} \tag{4}$$

Based on the Projection method, the implicit technique can be used to solve Eqs. (3) and (4).

Equations (3) and (4) can be rewritten in the form

$$\nabla\cdot\boldsymbol{u}^{n+1}=0 \tag{5}$$

$$\frac{\boldsymbol{u}^{n+1}}{\delta t}-\frac{1}{2Re}\nabla^2\boldsymbol{u}^{n+1}=\frac{\boldsymbol{u}^{n}}{\delta t}-\nabla\cdot(\boldsymbol{uu})^n-\nabla p^{n+1}+\frac{1}{2Re}\nabla^2\boldsymbol{u}^n+\frac{1}{Fr^2}\boldsymbol{g}^n \tag{6}$$

where δt is the time step increment; $\boldsymbol{u}=(u, v, w)$ and p can be obtained as follows:

Step 1 The basic opinion behind this approach is to use Eq. (6) to solve for the intermediate velocity field $\tilde{\boldsymbol{u}}=(\tilde{u},\tilde{v},\tilde{w})$.

$$\frac{\tilde{\boldsymbol{u}}}{\delta t}-\frac{1}{2Re}\nabla^2\tilde{\boldsymbol{u}}=\frac{\boldsymbol{u}^n}{\delta t}-\nabla\cdot(\boldsymbol{uu})^n-\nabla p^{n+1}+\frac{1}{2Re}\nabla^2\boldsymbol{u}^n+\frac{1}{Fr^2}\boldsymbol{g}^n \tag{7}$$

Equation (7) can be approximated as follows: the time term and viscous term are solved through Crank−Nicolson method; the pressure term is discretized using forward differences; the convective terms can be solved through the high order upwind scheme.

For example, the momentum equation, Eq. (7), is approximated by the following finite difference equation in the x direction.

$$\begin{aligned}&\left[1+\left(\frac{\delta t}{Re}\right)\left(\frac{1}{\delta x^2}+\frac{1}{\delta y^2}+\frac{1}{\delta z^2}\right)\right]\tilde{u}_{i+\frac{1}{2},j,k}-\\&\left(\frac{\delta t}{2Re\delta x^2}\right)\left(\tilde{u}_{i+\frac{3}{2},j,k}+\tilde{u}_{i-\frac{1}{2},j,k}\right)-\\&\left(\frac{\delta t}{2Re\delta y^2}\right)\left(\tilde{u}_{i+\frac{1}{2},j+1,k}+\tilde{u}_{i+\frac{1}{2},j-1,k}\right)-\\&\left(\frac{\delta t}{2Re\delta z^2}\right)\left(\tilde{u}_{i+\frac{1}{2},j,k+1}+\tilde{u}_{i+\frac{1}{2},j,k-1}\right)=\\&u^n_{i+\frac{1}{2},j,k}+\delta t\left[-\left(\frac{p_{i+1,j,k}-p_{i,j,k}}{\delta x}\right)^n+\frac{1}{Fr^2}g_x-\right.\\&\left(F_{UX}+F_{UY}+F_{UZ}\right)^n+\\&\frac{1}{2Re}\left(\frac{u_{i-\frac{1}{2},j,k}-2u_{i+\frac{1}{2},j,k}+u_{i+\frac{3}{2},j,k}}{\delta x^2}+\right.\\&\frac{u_{i+\frac{1}{2},j-1,k}-2u_{i+\frac{1}{2},j,k}+u_{i+\frac{1}{2},j+1,k}}{\delta y^2}+\\&\left.\left.\frac{u_{i+\frac{1}{2},j,k-1}-2u_{i+\frac{1}{2},j,k}+u_{i+\frac{1}{2},j,k+1}}{\delta z^2}\right)\right]\end{aligned} \tag{8}$$

$$F_{UX}=\frac{u_{i+\frac{1}{2},j,k}}{2}\cdot[D_{UL}+D_{UR}+\alpha\,\mathrm{sgn}(u_{i+\frac{1}{2},j,k})(D_{UL}-D_{UR})] \tag{9}$$

$$F_{UY}=\frac{v_{i+\frac{1}{2},j,k}}{2}\cdot[D_{UB}+D_{UT}+$$

$$\alpha \operatorname{sgn}(v_{i+\frac{1}{2},j,k})(D_{UB}-D_{UT})] \quad (10)$$

$$F_{UZ}=\frac{w_{i+\frac{1}{2},j,k}}{2}\cdot[D_{UQ}+D_{UH}+$$

$$\alpha \operatorname{sgn}(w_{i+\frac{1}{2},j,k})(D_{UQ}-D_{UH})] \quad (11)$$

where

$$D_{UL}=\frac{u_{i+\frac{1}{2},j,k}-u_{i-\frac{1}{2},j,k}}{\delta x};D_{UR}=\frac{u_{i+\frac{3}{2},j,k}-u_{i+\frac{1}{2},j,k}}{\delta x};$$

$$D_{UB}=\frac{u_{i+\frac{1}{2},j,k}-u_{i+\frac{1}{2},j-1,k}}{\delta y};D_{UT}=\frac{u_{i+\frac{1}{2},j+1,k}-u_{i+\frac{1}{2},j,k}}{\delta y};$$

$$D_{UQ}=\frac{u_{i+\frac{1}{2},j,k}-u_{i+\frac{1}{2},j,k-1}}{\delta z};D_{UH}=\frac{u_{i+\frac{1}{2},j,k+1}-u_{i+\frac{1}{2},j,k}}{\delta z};$$

$\operatorname{sgn}\left(u_{i+\frac{1}{2},j,k}\right)$ is equal to 1 if $u_{i+\frac{1}{2},j,k}>0$ and −1 if $u_{i+\frac{1}{2},j,k}<0$; $0<\alpha<1$. Other parameters can be treated similarly. The z- and y-component of the momentum equations can be solved in the same way.

Step 2 The velocity field can be written as the following form by the Helmholtz-Hodge method.

$$\begin{cases}u^{n+1}=\tilde{u}-\delta t\dfrac{\partial \psi^{n+1}}{\partial x}\\ v^{n+1}=\tilde{v}-\delta t\dfrac{\partial \psi^{n+1}}{\partial y}\\ w^{n+1}=\tilde{w}-\delta t\dfrac{\partial \psi^{n+1}}{\partial z}\end{cases} \quad (12)$$

Taking the divergence of Eq. (12) and imposing the mass conservation for $\boldsymbol{u}^{n+1}=(u^{n+1},v^{n+1},w^{n+1})$, the Poisson equation was obtained for ψ^{n+1}.

$$\nabla^2\psi^{n+1}=(1/\delta t)\nabla\cdot\tilde{\boldsymbol{u}} \quad (13)$$

This equation can be solved in fluid region and is applied to all full cells. The Poisson equation for ψ^{n+1} on the free surface can be found in results by TOME et al [17−20].

Step 3 To obtain the equation for the pressure, $\tilde{\boldsymbol{u}}$ is introduced from Eq. (12) into Eq. (7) and then subtracting it from Eq. (6), the following equation can be obtained.

$$p^{n+1}=p^n+\psi^{n+1}-\frac{\delta t}{2Re}\nabla^2\psi^{n+1} \quad (14)$$

After $\psi^{n+1}_{i,j,k}$ was calculated for all full cells, the pressure field is approximated by the following finite difference equation.

$$p^{n+1}_{i,j,k}=p^n_{i,j,k}+\psi^{n+1}_{i,j,k}-\frac{\delta t}{2Re}\cdot\left(\frac{\psi^{n+1}_{i+1,j,k}-2\psi^{n+1}_{i,j,k}+\psi^{n+1}_{i-1,j,k}}{\delta x^2}+\frac{\psi^{n+1}_{i,j+1,k}-2\psi^{n+1}_{i,j,k}+\psi^{n+1}_{i,j-1,k}}{\delta y^2}+\frac{\psi^{n+1}_{i,j,k+1}-2\psi^{n+1}_{i,j,k}+\psi^{n+1}_{i,j,k-1}}{\delta z^2}\right) \quad (15)$$

Finally, the intermediate velocity field $\tilde{\boldsymbol{u}}=(\tilde{u},\tilde{v},\tilde{w})$ is calculated from Eq. (7) and the velocity field $\boldsymbol{u}=(u,v,w)$ is calculated from Eq. (12). The pressure field is calculated from Eq. (15).

The liquid metal containing solid grains and being at lower temperature is treated as incompressible non-Newtonian flow. According to Eq. (1) and Eq. (2), the general mathematical equations of the liquid metal containing solid grains can be written as

$$\nabla\cdot\boldsymbol{u}=0 \quad (16)$$

$$\frac{\partial\boldsymbol{u}}{\partial t}+\nabla\cdot(\boldsymbol{uu})=-\nabla p+\frac{\lambda_2}{\lambda_1}\frac{1}{Re}(\nabla^2\boldsymbol{u})+\nabla\cdot\boldsymbol{S}+\frac{1}{Fr^2}\boldsymbol{g} \quad (17)$$

There are some methods to solve Eq. (16) and Eq. (17) using implicit techniques [18−21]. If the Crank−Nicolson method is used for the viscous term, Eq. (16) and Eq. (17) can be written as

$$\nabla\cdot\boldsymbol{u}^{n+1}=0 \quad (18)$$

$$\frac{\boldsymbol{u}^{n+1}}{\delta t}-\frac{\lambda_2}{\lambda_1}\frac{1}{2Re}\nabla^2\boldsymbol{u}^{n+1}=\frac{\boldsymbol{u}^n}{\delta t}-\nabla\cdot(\boldsymbol{uu})^n-\nabla p^{n+1}+\frac{\lambda_2}{\lambda_1}\frac{1}{2Re}\nabla^2\boldsymbol{u}^n+\nabla\boldsymbol{S}^n+\frac{1}{Fr^2}\boldsymbol{g}^n \quad (19)$$

The solving process of incompressible non-Newtonian flow is similar to the previous solving process of incompressible Newtonian flow. $\boldsymbol{u}=(u,v,w)$ and p can be obtained as follows.

Step 1 Eq. (19) is solved for the provisional velocity field $\tilde{\boldsymbol{u}}=(\tilde{u},\tilde{v},\tilde{w})$.

$$\frac{\tilde{\boldsymbol{u}}}{\delta t}-\frac{\lambda_2}{\lambda_1}\frac{1}{2Re}\nabla^2\tilde{\boldsymbol{u}}=\frac{\boldsymbol{u}^n}{\delta t}-\nabla\cdot(\boldsymbol{uu})^n-\nabla p^n+\frac{\lambda_2}{\lambda_1}\frac{1}{2Re}\nabla^2\boldsymbol{u}^n+\nabla\boldsymbol{S}^n+\frac{1}{Fr^2}\boldsymbol{g}^n \quad (20)$$

Step 2 Using Helmholtz−Hodge theory, the velocity field $\boldsymbol{u}^{n+1}=(u^{n+1},v^{n+1},w^{n+1})$ can be decomposed as

$$\boldsymbol{u}^{n+1}=\tilde{\boldsymbol{u}}-\delta t\nabla\psi^{n+1} \quad (21)$$

Step 3 The pressure field is calculated from the following equation.

$$p^{n+1} = p^n + \psi^{n+1} - \frac{\lambda_2}{\lambda_1}\frac{\delta t}{2Re}\nabla^2\psi^{n+1} \tag{22}$$

where $\nabla^2\psi^{n+1} = (1/\delta t)\nabla\cdot\tilde{\boldsymbol{u}}$ and the non-Newtonian stress tensor $\boldsymbol{S}$ can be calculated from the Oldroyd−B constitutive equation [17−19].

$$\frac{\partial \boldsymbol{S}}{\partial t} = -(\boldsymbol{u}^{n+1}\cdot\nabla)\boldsymbol{S} + (\nabla\boldsymbol{u}^{n+1})^{\mathrm{T}}\boldsymbol{S} + \boldsymbol{S}(\nabla\boldsymbol{u}^{n+1}) + \frac{1}{We}\left[\frac{1}{Re}\left(1-\frac{\lambda_2}{\lambda_1}\right)((\nabla\boldsymbol{u}^{n+1}) + (\nabla\boldsymbol{u}^{n+1})^{\mathrm{T}}) - \boldsymbol{S}\right] \tag{23}$$

3 Level set method

In mold filling processes, the interface boundary between the gas and the liquid metal may have severe topological changes, such as interface pinching and breaking. These problems can be solved through Level set method [16−18]. In Level set method, the Level set function $\varphi(\boldsymbol{x}, t)$ is defined as the distance of the mesh center to the interface boundary (φ=0 on the interface boundary Ω_{boundary}, φ>0 in the air region Ω_{air} and φ<0 in the liquid region Ω_{liouid}). The Level set function $\varphi(\boldsymbol{x}, t)$ can be written as

$$\varphi(\boldsymbol{x},t) = \begin{cases} d(\boldsymbol{x},\Omega), & x\in\Omega_{\text{air}} \\ 0, & x\in\Omega_{\text{boundary}} \\ -d(\boldsymbol{x},\Omega), & x\in\Omega_{\text{liquid}} \end{cases} \tag{24}$$

Since the interface boundary moves, the transient evolution of the interface boundary can be described with Hamilton−Jacobi equation.

$$\frac{\partial\varphi}{\partial t} + \bar{V}\cdot(\nabla\varphi) = 0 \tag{25}$$

where $\bar{V} = (u, v, w)$ is the interface boundary propagating velocity that can be set as local liquid metal fluid /gas fluid velocity. Equation (25) can be rewritten as

$$\frac{\partial\varphi}{\partial t} = -u\frac{\partial\varphi}{\partial x} - v\frac{\partial\varphi}{\partial y} - w\frac{\partial\varphi}{\partial z} = L(\varphi) \tag{26}$$

where the spatial derivative of Eq. (26) is approximated by the fifth order weighted essentially non-Oscillatory (WENO) method and the time derivative of Eq. (26) is approximated by the second order Runge−Kutta method [16−18].

Even if $\varphi(\boldsymbol{x}, t)$ can be initialized as a signed distance from the interface boundary, it may not remain the distance function due to repeated iteration. The re-initialization methods can be used to keep $\varphi(\boldsymbol{x}, t)$ as the distance function. One of the effective methods is to solve the following equations. Once φ is got, the interface boundary is also known.

$$\begin{cases} \dfrac{\partial\varphi}{\partial t} = \operatorname{sgn}(\varphi_0)(1-|\nabla\varphi|) \\ \varphi(\boldsymbol{x},0) = \varphi_0 \end{cases} \tag{27}$$

4 Results and discussion

In the work, a finite difference-based interface Projection-Level set method is developed for gas−liquid two-phase mold filling simulation in casting. The governing equations for incompressible Newtonian flow and incompressible non-Newtonian flow are solved through projection method. The Level set method is used to track the gas−liquid interface boundary.

Finally, a new program is developed based on the Projection-Level set method. The outline of this program can be described as follows. 1) The value of (u^n, v^n, w^n), p^n and φ^n at all cells are initialize. 2) The governing equations for incompressible Newtonian flow and incompressible non-Newtonian flow are solved through projection method, and hence (u^{n+1}, v^{n+1}, w^{n+1}) and p^{n+1} can be obtained. 3) Eq. (26) is solved to get the value of φ^{n+1} in the next time step. 4) The Level set is re-initialized to keep φ^{n+1} as the distance function. 5) Go to (2) for the next time step.

In order to demonstrate the correctness of this new program for simulation of gas−liquid two-phase mold filling in casting, a benchmark filling experiment is simulated. The benchmark test was designed by XU et al [25] and the filling process was recorded by a 16-mm film camera. Most of their details are similar to previous experiments [24−26].

The casting is a plate of 400 m×400 mm×20 mm and the gating system is shown in Fig. 1. The 3D model is shown in Fig. 2. The physical parameters of the casting and mold are shown in Table 1 and Table 2. The pouring speed is 0.7 m/s and the pouring temperature is 700 °C.

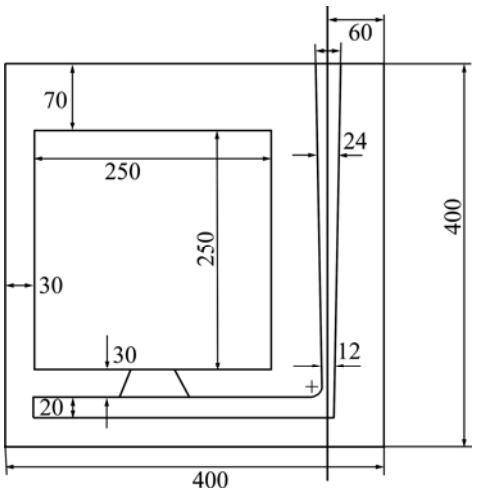

Fig. 1 Gating system (Unit: mm)

Table 1 Physical parameters of casting

Material	Specific latent/ ($kJ \cdot kg^{-1}$)	Density/ ($kg \cdot m^{-3}$)	Specific heat capacity/ ($kJ \cdot kg^{-1} \cdot K^{-1}$)	Solidus temperature/ °C	Liquidus temperature/ °C
Aluminum	397.5	2315−2702	0.9−1.09	655	663

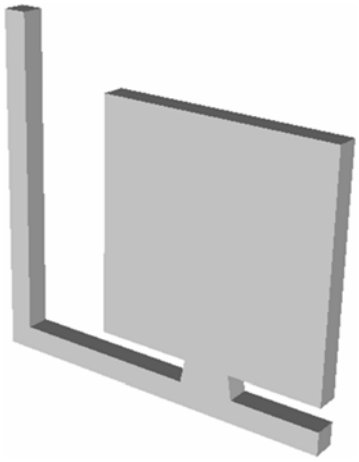

Fig. 2 3D model of mold

Table 2 Physical parameters of mold

Material	Density/ ($kg \cdot m^{-3}$)	Specific heat capacity/ ($kJ \cdot kg^{-1} \cdot K^{-1}$)
Sand	2780	0.54−1.00

In numerical calculation, the mesh dimensions are 2.0 mm×2.0 mm×2.0 mm. Figure 3 shows the mesh model. The new program based on the Projection−Level set method is used to simulate the filling process. Figure 4 shows the comparison between the simulated and experimental results.

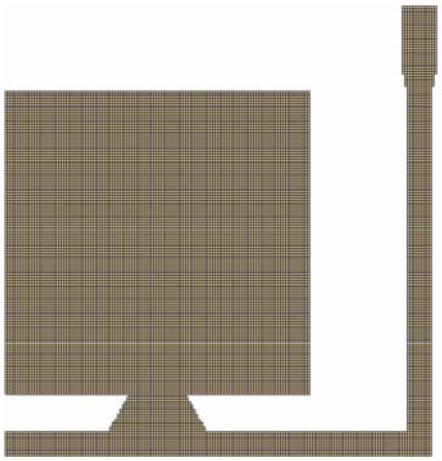

Fig. 3 Original mesh of model

The simulated and experimental results are illustrated in Fig. 4. which were captured with the high speed 16 mm camera at 0.83, 1.43, 1.93, 2.37 and 2.51 s; whereas other sub-figures are the corresponding simulated results. The simulated results agree very well with the experimental results. It is clear that this new program based on the Projection−Level set method can be used to properly predicate the gas−liquid two-phase mold filling simulation in casting.

Statistical analyses [27−30] are given to further demonstrate the correctness of this new program. The process can be described as follows. 1) The simulation results of filling process of the same aluminum casting are calculated by the new program and the SOLA-VOF method [15] (the SOLA method is often used to solve the velocity and pressure of the thermal flow filling process). The results of the velocity field and pressure field are compared at different time points (1.0, 2.0, and 3.0 s). 2) The case of the velocity in x direction at 1.0 s is taken. The sample is all meshes except boundary. The Wilcoxon signed rank test is used and the calculated results are listed in Table 3, where the last two rows are the ranks. The absolute rank row has no signs, and the signed rank row gives the ranks along with their sign [27−30].

Table 3 Calculation results of velocity in x direction at 1.0 s

Subject	X_1	X_2	X_3	X_4	…
SOLA-VOF method (x_i)	−0.001421	0.002384	0.006152	−0.003006	…
This new program (y_i)	−0.001433	0.002387	0.006152	−0.003031	…
$D_i=\|x_i-y_i\|$	0.000012	0.000003	0	0.000025	…
Absolute rank	1041.02	67.5	−	2571.1	…
Signed rank	1041.02	−67.5	−	2571.1	…

X_i represents the meshes; x_i represents the velocities calculated by the SOLA-VOF method; y_i represents the velocities calculated by this new program.

The following null and alternative hypotheses are used:

H0: the simulation results are unanimous between this new program and the SOLA-VOF method.

H1: the simulation results are not unanimous between this new program and the SOLA-VOF method.

The test statistic is given in Refs. [27−30].

$$-1.6449 < T = \sum_{i=1}^{n} R_i \Big/ \sqrt{\sum_{i=1}^{n} R_i^2} = 0.6719 < 1.6449 \quad (\alpha = 0.1) \tag{28}$$

There is no enough evidence to reject H0. Other analyses are similar at 2.0, and 3.0 s. Analysis shows

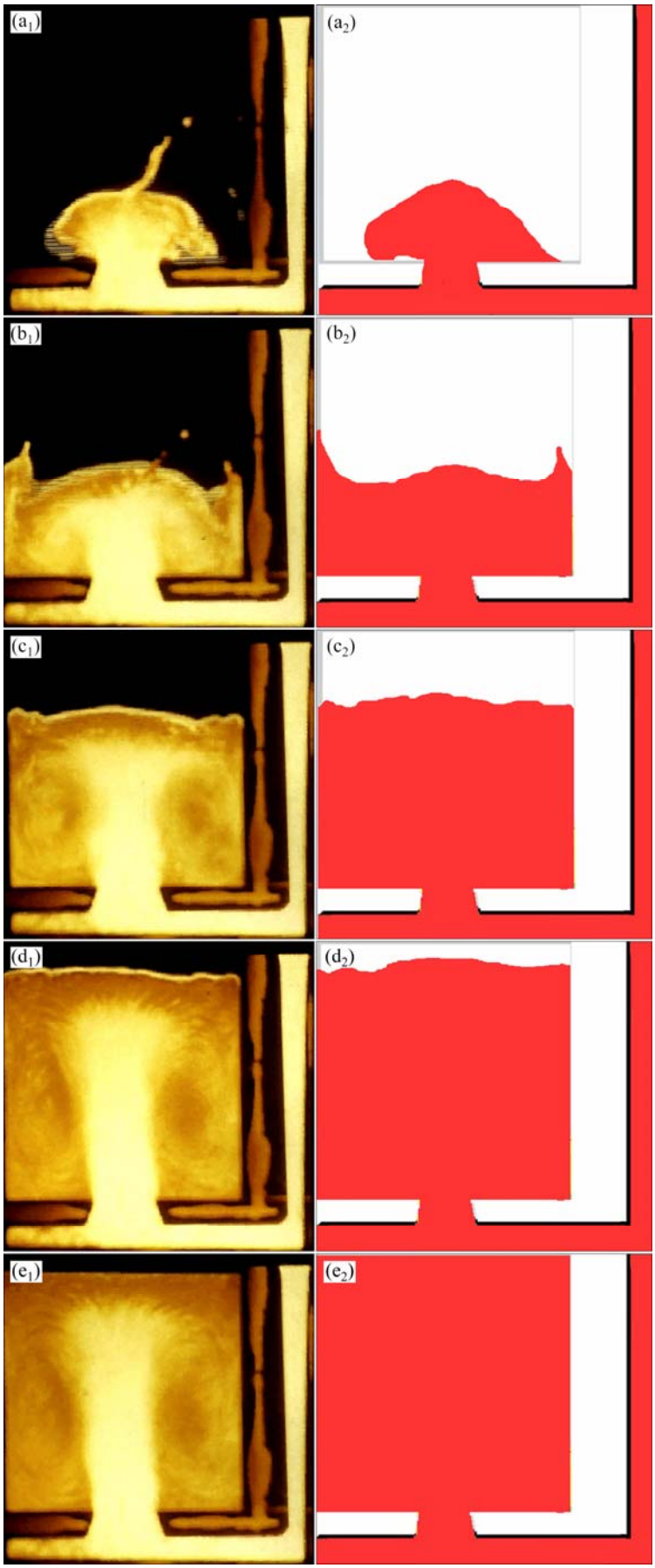

Fig. 4 Comparison between simulated (left) and experimental (right) results: (a_1, a_2) 0.83 s; (b_1, b_2) 1.43 s; (c_1, c_2) 1.93 s; (d_1, d_2) 2.37 s; (e_1, e_2) 2.51 s

that the simulation results are unanimous between this new program and the SOLA-VOF method. It is proved that this new program is correct.

The comparison results of calculating time are shown in Table 4.

Table 4 Computing time

Method	Mesh	Computing time/s
SOLA-VOF method	2.0 mm×2.0 mm×2.0 mm	1203
This new program	2.0 mm×2.0 mm×2.0 mm	762

As illustrated in Table 4, the new program reduces calculating time by 35%. It is true that the new program calculates more quickly than the SOLA-VOF method.

5 Conclusions

1) A three-dimensional interface Projection−Level numerical model considering characteristics of liquid metal is proposed for simulating the gas−liquid flow problems during casting's mould filling process. The governing equations for incompressible Newtonian flow and incompressible non-Newtonian flow are solved through the Projection method. The Level set method is used to track the gas−liquid interface boundary. This model allows to properly predicate the gas motion, the liquid motion, and the reciprocal effect of the two phases; specifically, this model can be used to properly predicate the gas entrapment defects. Finally, a new program is developed for gas−liquid two-phase mold filling simulation in casting.

2) In order to demonstrate the correctness of the new program for simulation of gas−liquid two-phase mold filling in casting, a benchmark filling experiment is simulated. The simulated results show that the new program can be used to properly predicate the gas−liquid two-phase mold filling simulation in casting; this new program is more quickly than the SOLA-VOF method.

References

[1] WANG Y Q, ALI N, HAYAT T, OBERLACK M. Peristaltic motion of a magnetohydrodynamic micropolar fluid in a tube [J]. Applied Mathematical Modelling , 2011, 35(8): 3737−3750.

[2] WANG Y Q, HAYAT T, ALI N, OBERLACK M. Magnetohydrodynamic peristaltic motion of a Sisko fluid in a symmetric or asymmetric channel [J]. Physica A: Statistical Mechanics and its Applications, 2008, 387(2): 347−362.

[3] HE Yi, ZHOU Zhao-yao, CAO Wen-jiong, CHEN Wei-ping. Simulation of mould filling process using smoothed particle hydrodynamics [J]. Transactions of Nonferrous Metals Society of China, 2011, 21: 2684−2692.

[4] LI Ming-ming, LUO Ji-xiang, LUO Guo-jian, CHEN Yun, XIE Wei-lian. Squeeze casting technics numerical simulation of spray-gun [J]. Journal of Wuhan University of Technology, 2010, 32(15): 76−79. (in Chinese)

[5] LUO Ji-xiang, HU Jia-hua, CHEN Wei, BAI Xu-bai. The study on the filling type of metal liquid in squeeze casting [J]. Journal of Wuhan University of Technology, 2003, 25(2): 23−26. (in Chinese)

[6] MIRBAGHERI S M H, SHRINPARVAR M, ASHORY H, DAVAMI P. Simulation of surface roughness on the flow pattern in the casting process [J]. Materials & Design, 2004, 25: 655−661.

[7] GUAN Ren-guo, ZHAO Zhan-yong, CHAO Run-ze, LIAN Chao, WEN Jing-lin. Simulation of temperature field and metal flow during continuous semisolid extending extrusion process of 6201 alloy tube [J]. Transactions of Nonferrous Metals Society of China, 2012, 22: 1182−1189.

[8] SHI Fei, DONG Xiang-huai. 3D numerical simulation of filling and curing processes in non-isothermal RTM process cycle [J]. Finite Elements in Analysis and Design, 2011, 47: 764−770.

[9] YANG Bin-xin, OUYANG Jie, LI Xue-juan. Simulation of fiber reinforced composite materials mold filling process and mechanical properties analysis [J]. Journal of Non-Newtonian Fluid Mechanics, 2011, 166: 1129−1136.

[10] CHEN Ye, ZHAO Yu-hong, HOU Hua. Numerical simulation for thermal flow filling process casting [J]. Transactions of Nonferrous Metals Society of China, 2006, 16: 214−218.

[11] SONG Nan-nan, LUAN Yi-kun, BAI Yun-long, KANG Xiu-hong, XIA Li-jun, LI Dian-zhong. Computer simulation of core filling process of cast high speed steel roll [J]. China Foundry, 2009, 6(4): 314−318.

[12] NIU Xiao-feng, LIANG Wei, ZHAO Yu-hong, HOU Hua, MU Yang-qing. A new implicit finite difference algorithm of thermal melt flow in filling process based on projection method [J]. Journal of Computational and Theoretical Nanoscience, 2012, 9: 1374−1378.

[13] NIU Xiao-feng, LIANG Wei, ZHAO Yu-hong, HOU Hua, MU Yan-qing, HUANG Zhi-wei. New algorithm for solving 3D incompressible viscous equations based on projection method [J]. Transactions of Nonferrous Metals Society of China, 2011, 21: 1826−1832.

[14] ZHAO Hai-dong, BAI Yan-fei, OUYANG Xiao-xian. Simulation of mold filling and prediction of gas entrapment on practical high pressure die castings [J]. Transactions of Nonferrous Metals Society of China, 2010, 20(11): 2064−2070.

[15] HOU Hua. Studies on numerical simulation for liquid-metal filling and solidification during casting process [D]. Saitama: Saitama Institute of Technology, 2005: 43−69.

[16] CHENADEC V L, PITSCH H. A 3D Unsplit forward/backward volume-of-fluid approach and coupling to the level set method [J]. Journal of Computational Physics, 2013, 233(15): 10−33.

[17] OISHI C M, TOME M F, CUMINATO J A, MCKEE S. An implicit technique for solving 3D low Reynolds number moving free surface flows [J]. Journal of Computational Physics, 2008, 227(16): 7446−7468.

[18] TOME M F, CASTELO A, FERREIRA V G, MCKEE S. A finite difference technique for solving the Oldroyd-B model for 3D-unsteady free surface flows [J]. Journal of Non-Newtonian Fluid Mechanics, 2008, 154 (2): 179−206.

[19] TOME M F, MANGIAVACCHI N, CUMINATO J A, CASTELO A, MCKEE S. A finite difference technique for simulation unsteady viscoelastic free surface flows [J]. Journal of Non-Newtonian Fluid Mechanics, 2002, 106 (2): 61−106.

[20] TOME M F, GROSSI L, CASTELO A, CUMINATO J A, MCKEE S, WALTERS K. Die-swell, splashing drop and a numerical technique for solving the Oldroyd-B model for axisymmetric free surface flows [J]. Journal of Non-Newtonian Fluid Mechanics, 2007, 141(2): 148−166.

[21] LIU Hui-po, YAN Ning-ning. Enhancing finite element approximation for eigenvalue problems by projection method [J].

Computer Methods in Applied Mechanics and Engineering, 2012, 233: 81−91.

[22] HE Hong-jin, HAN De-ren, LI Zhi-bao. Some projection methods with the BB step sizes for variational inequalities [J]. Journal of Computational and Applied Mathematics, 2012, 236(9): 2590−2604.

[23] FIROOZABADI B, MAHDINIA M. 2D numerical simulation of density currents using the SPH projection method [J]. European Journal of Mechanics B: Fluids, 2013, 38: 38−46.

[24] SAN O, STAPLES A E. A coarse-grid projection method for accelerating incompressible flow computations [J]. Journal of Computational Physics, 2013, 233(15): 480−508.

[25] XU Zhi-an, MAMPAEY F. Experimental and simulation study on mold filling coupled with heat transfer [J]. AFS Trans, 1994, 102: 181−188.

[26] SIRRELL B, HOLLIDAY M, CAMPBELL J. Benchmark testing the flow and solidification modeling of Al castings [J]. The Member Journal of TMS, 1996, 48(3): 20−23.

[27] DERRAC J, GARCIA S, MOLINA D, HERRERA F. A practical tutorial on the use of nonparametric statistical tests as a methodology for comparing evolutionary and swarm intelligence algorithms [J]. Swarm and Evolutionary Computation, 2011, 1(1): 3−18.

[28] GOSPODINOY N, HIRUKAWA M. Nonparametric estimation of scalar diffusion models of interest rates using asymmetric kernels [J]. Journal of Empirical Finance, 2012, 19(4): 595−609.

[29] CONOVER W J. Practical nonparametric statistics [M]. Hoboken: Wiley Publishing Inc, 2006: 194−207.

[30] ABELLAN J, BAKER R M, COOLEN F P A, CROSSMAN R J. Classification with decision trees from a nonparametric predictive inference perspective [J]. Computational Statistics & Data Analysis, 2013, 27: 1−14.

基于充型过程金属液流动特点的气–液两相流算法模型

牛晓峰[1]，方 钊[2]，梁 伟[1]，侯 华[3]，王红霞[1]

1. 太原理工大学 材料科学与工程学院，太原 030024；
2. 西安建筑科技大学 冶金工程学院，西安 710055；
3. 中北大学 材料科学与工程学院，太原 030051

摘 要：针对在铸件充型过程中，金属液表现出不同的流动特点，含有固体颗粒的金属液具有不可压缩非牛顿流的流动特性，而过热金属液具有不可压缩牛顿流的流动特点，采用 Projection 方法求解气体、过热金属液和含有固体颗粒的金属液的速度场，用 Level set 方法来追踪气−液界面边界。为了验证计算模型，将模拟结果与实验结果(采用 16 mm 摄像机记录充型过程)进行比对，从而证明计算模型的正确性。

关键词：有限差分法；充型过程；Projection 方法；Level set 方法；两相流；数值模拟

(Edited by Hua YANG)